INL/EXT-10-20275

Testing of Small Graphite Samples for Nuclear Qualification

Julie Chapman

November 2010

The INL is a U.S. Department of Energy National Laboratory
operated by Battelle Energy Alliance

INL/EXT-10-20275

Testing of Small Graphite Samples for Nuclear Qualification

Julie Chapman

November 2010

Idaho National Laboratory
Next Generation Nuclear Plant
Idaho Falls, Idaho 83415

http://www.inl.gov

Prepared for the
U.S. Department of Energy
Office of Nuclear Energy
Under DOE Idaho Operations Office
Contract DE-AC07-05ID14517

PHOTOCOPY AND USE AUTHORIZATION

In presenting this thesis in partial fulfillment of the requirements for an advanced degree at Idaho State University, I agree that the Library shall make it freely available for inspection. I further state that permission for extensive copying of my thesis for scholarly purposes may be granted by the Dean of the Graduate School, Dean of my academic division, or by the University Librarian. It is understood that any copying or publication of this thesis for financial gain shall not be allowed without my written permission.

Signature_____

Date_____

TESTING OF SMALL GRAPHITE SAMPLES FOR NUCLEAR QUALIFICATION

by

Julie A. Chapman, B.S.

A thesis

submitted in partial fulfillment

of the requirements for the degree of

Master of Science in Nuclear Science and Engineering

Idaho State University

November 2010

COMMITTEE APPROVAL

To the Graduate Faculty:

The members of the committee appointed to examine the thesis of JULIE CHAPMAN find it satisfactory and recommend that it be accepted.

Dr. Mary Lou Dunzik-Gougar,
Major Advisor

Dr. Eric Burgett
Committee Member

Dr. William Windes
Committee Member

Dr. Daniel Dale,
Graduate Faculty Representative

CONTENTS

FIGURES

TABLES

ACRONYMS

AGC-1	Advanced Graphite Capsule 1
ANOVA	Analysis of Variance
ASTM	American Society for Testing and Materials
ATR	Advanced Test Reactor
CP-1	Chicago Pile 1
HCP	Hexagonal Close Packed
HOPG	Highly Oriented Pyrolytic Graphite
HTGR	High Temperature Gas-cooled Reactor
INL	Idaho National Laboratory
MPa	Mega Pascals
NBG-18	Nuclear Block Grade 18 (Graphite)
NGNP	Next Generation Nuclear Plant
SGL	SGL Group (A graphite manufacturer)
TRISO	Tri-Isotopic (Fuel)
VHTR	Very High Temperature Reactor

ABSTRACT

Accurately determining the mechanical properties of small irradiated samples is crucial to predicting the behavior of the overall irradiated graphite components within a Very High Temperature Reactor. The sample size allowed in a material test reactor, however, is limited, and this poses some difficulties with respect to mechanical testing. In the case of graphite with a larger grain size, a small sample may exhibit characteristics not representative of the bulk material, leading to inaccuracies in the data.

A study to determine a potential diameter effect on the stress at sample failure was pursued under the Next Generation Nuclear Plant program. A 21.7% reduction in diameter (from eight to six grains) led to a 12.7% reduction in failure stress. A 37.0% reduction in diameter (from eight to five grains) led to a 14.8% reduction in failure stress. An effect on the failure stress from reducing the sample diameter was successfully identified.

1. Introduction

1.1 The NGNP Mission and History

The Next Generation Nuclear Plant (NGNP) had its beginnings in a document authored by the Department of Energy's Nuclear Energy Research Advisory Committee in cooperation with the Generation IV International Forum. This document, *A Technology Roadmap for Generation IV Nuclear Energy Systems*, was published in December of 2002. The NGNP project was formally established by the Energy Policy Act of 2005, (Public Law 109-58, 42 USC 16021) (DOE-NE 2010).

The NGNP project focus is design and construction of a nuclear power plant that would generate both hydrogen and electricity. The basis for the NGNP design is a high temperature gas-cooled reactor (HTGR) such as a helium-cooled prismatic or pebble-bed, graphite-moderated reactor using low-enriched uranium, tri-isotopic (TRISO) coated fuel (T. Burchell, R. L. Bratton, et al. 2007).

The mission of the NGNP Materials Research and Development program is to provide the necessary research and development of materials to support the design and licensure of the reactor and balance of plant, excluding a potential hydrogen plant (Idaho National Laboratory 2008).

The program consists of metal, graphite, and ceramic composite areas of research. The Graphite program focuses on determining the material properties and behavior of graphite for use as a nuclear core component material. Particulars of the research involve the thermal, physical, and mechanical properties of interest for nuclear graphite. Properties such as thermal conductivity, thermal expansion, elastic modulus,

microstructure, and strength are being measured for the new nuclear grade graphites of interest to the NGNP program.

The Graphite program consists of three branches: the irradiation program, the baseline program, and the mechanisms program. The irradiation program focuses on studying irradiated graphite and associated phenomena attributed to graphite irradiation including material property changes due to irradiation. The baseline program studies as-fabricated, unirradiated properties of graphite. The mechanisms development program focuses on the scientific explanations and analytical models for phenomena that occur in graphite. These three branches together help achieve the overall mission of the NGNP program.

1.2 The History and Development of Graphite

The first use of graphite as a neutron moderator in a nuclear reactor was in Chicago Pile 1 (CP-1) in December of 1942. Since that time, graphite has been used both as a structural material and as a moderator in several reactors such as the Albeitsgemeinschaft Versuchsreaktor, Reactor Bolshoi Moschnosti Kanalynyi, and the Fort St. Vrain reactor (Windes, Burchell and Bratton 2007). Now it is being researched and developed for use in the NGNP. For the NGNP, graphite will serve as a neutron moderator as well as a major structural component of the reactor. A schematic of a candidate reactor design is shown in Figure 1. A graphite component of a Pebble Bed Modular Reactor is shown in Figure 2.

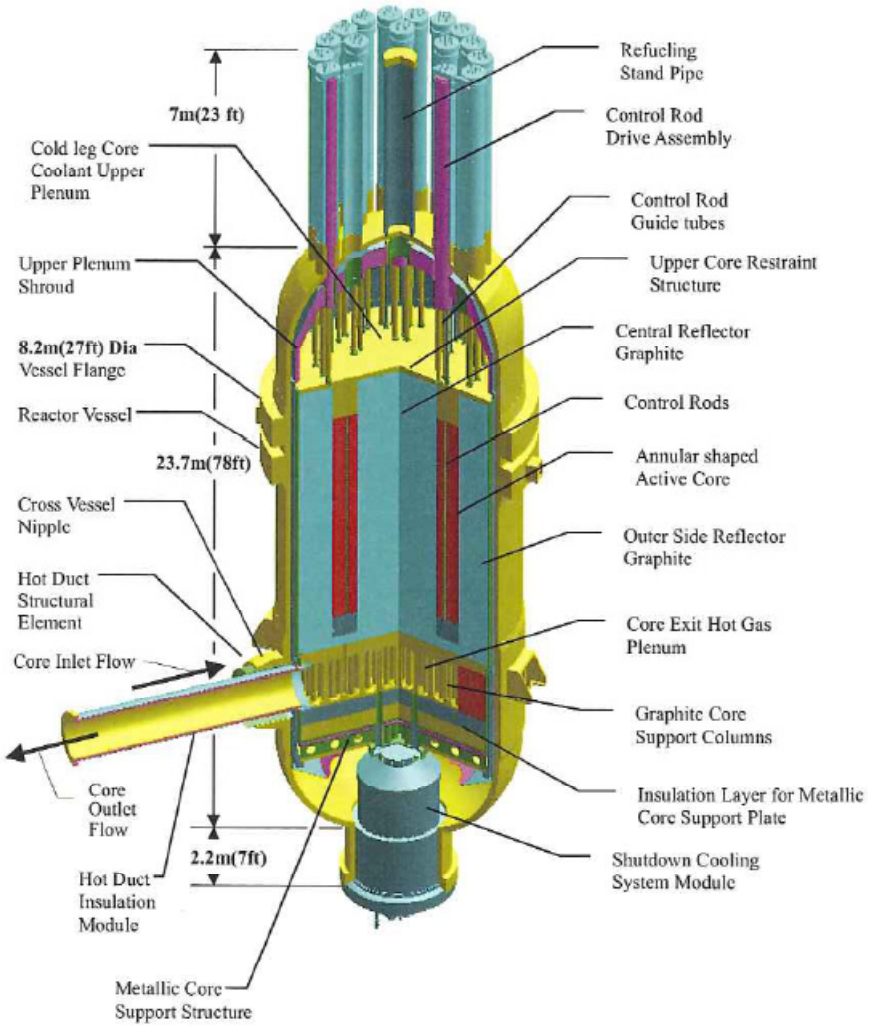

Figure 1: A schematic of a HTGR showing the graphite constituents of the core (Idaho National Laboratory 2008).

Figure 2: Pebble Bed Modular Reactor demonstration power plant graphite test parts assembly (Burchell, Bratton and Windes, NGNP Graphite Selection and Acquisition Strategy 2007).

Previously characterized graphite grades used in the past no longer exist so new graphite grades have been developed. These new grades must be thoroughly characterized before they are qualified for use in the NGNP. The established baseline design of the NGNP provides guidance on expected doses and operation service lifetimes for the core graphite. Candidate materials must, therefore, be chosen and characterized accordingly (Windes, Burchell and Bratton 2007).

Graphite has undergone several iterations with different precursor materials. A needle coke graphite grade known as AGOT was used in the Hanford Piles and achieved some undesirable results. Needle coke is anisotropic and characterized by large optical domains and long acicular cracks and pores (T. Burchell 2007). Needle coke has its pregraphitic structure aligned along the major axis of the coke particle and therefore displays anisotropic behavior (T. Burchell 2007). When this anisotropic graphite undergoes irradiation, it does not react isotropically but rather develops large internal stresses in one direction, which results in cracking and a decreased irradiation lifetime. Isotropic cokes are favored for nuclear graphite applications because isotropy is crucial in predicting irradiation damage mechanisms.

1.3 Graphite Testing for the NGNP Project

An extensive NGNP Graphite Technology Development plan defines the testing to be performed for the chosen graphite candidates. Testing of both unirradiated and irradiated samples is crucial to defining operating parameters of the graphite in the NGNP. Samples currently being irradiated in the ATR at the Idaho National Laboratory are the first of a series to be irradiated for this program. The first set of samples will be examined for irradiation creep as well as irradiation effects on properties such as tensile strength, resistivity, modulus, and strain to failure. Data collected from these tests will be compared to pre-irradiation properties as well as NGNP design requirements.

The size and geometry of a reactor dictates sizes of irradiation samples and sample assemblies. The Advanced Graphite Capsule-1 (AGC-1) irradiation capsule, which contains the first set of NGNP samples, is no exception to this rule. Samples in the AGC-1 assembly are limited to a diameter of one-half inch and a length of one inch.

These small samples do not have the prerequisite geometry for standard mechanical testing procedures. The American Society for Testing and Materials (ASTM) has developed a method to tensile test samples of this configuration. This special method is described in Annex 4 of ASTM Standard C 781-08 (Standard Practice for Testing Graphite and Boronated Graphite Materials for High-Temperature Gas-Cooled Nuclear Reactor Components). The method states that a small graphite sample that is right circular cylindrical in geometry may be bonded to connectors that will connect to the load train designed for full size graphite specimens, as detailed in ASTM Standard C 749-08 (Standard Test Method for Tensile Stress-Strain of Carbon and Graphite). Although the method for small sample testing is detailed in ASTM C 781-08, there are no adhesives or

connectors specified for the application; therefore, different adhesives and connecting methods must be researched for this application.

It is not known whether such a small specimen will accurately represent the bulk material properties of the graphite. A certain kind of graphite known as Nuclear Block Grade-18 (NBG-18) has an average grain diameter of 1.6 mm. A full size ASTM graphite tensile specimen has a diameter of five-eighths of an inch (15.875 mm) , which on average has nine or ten grains across the diameter. A specimen that is one half inch in diameter (12.70 mm) will on average have seven or eight grains across the diameter. Whether or not the reduced number of grains affects the tensile stress at which the graphite fractures is the focus of the study presented in this thesis.

The key to defining experiments that produce useful data for NGNP graphite qualification is to incorporate sample size and geometry that will accommodate irradiation space availability while also retaining bulk material properties.

1.4 Thesis Objective

At issue for the research described in this thesis is the use of graphite samples that are smaller than the minimum size and geometry allowed by the ASTM standard for graphite tensile strength testing. Graphite samples may become less representative of the bulk material as the number of grains across the sample diameter decreases. The difference between bulk properties and single granular properties would be demonstrated in a change of stress required to fracture the sample.

Graphite has a multitude of cracks given its manufacture and structure. As the diameter of a sample reduces, the larger the cracks are with respect to the sample. These cracks can serve as stress concentrators as well as sites of flaw propagation and crack growth and could potentially amplify a smaller stress condition.

As the sample diameter decreases, so does the number of grains across that dimension; however, identically sized samples of different graphites may also have different numbers of grains. It is unknown whether the transition from bulk to single granular properties occurs at some threshold value, or across a range of decreasing grain number values. The objective of this work, therefore, is to determine the relationship, if any, between the number of graphite grains across the sample diameter and the tensile strength of the sample.

2. Review of Literature

2.1 Introduction to Graphite

By strict definition, graphite crystals are ideal, flawless materials with hexagonal crystal structures. However, the term is commonly used in reference to any material with a graphitic structure. In this thesis, the common definition will be used.

Graphite is the most stable allotrope of carbon at room temperature. Graphite consists of sheets with covalently bonded carbon atoms that are in a hexagonal configuration. In this configuration, carbon is hybridized in a sp^2 arrangement and has four valence electrons. Three of these valence electrons create sigma-bonds to the neighboring carbon atoms in a trigonal planar configuration whereas the fourth electron is delocalized and participates in covalent pi-bonding between the sheets of carbon atoms (called graphene planes), which is shown in Figure 3.

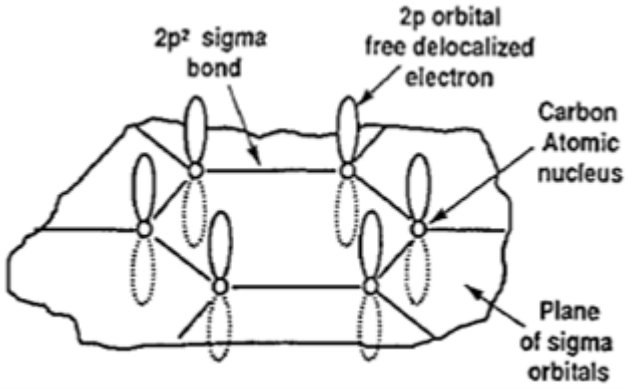

Figure 3: Diagram of the sp^2 hybridized configuration of graphite (Pierson 1993).

This electron delocalization makes graphite an aromatic structure and also serves to stabilize the in-plane bonding as the bond lengths are shorter and stronger than a traditional carbon-carbon sigma bond (Chung 2002). This delocalized electron also

makes graphite a conductor in-plane and an insulator out-of-plane. Graphite is a semi-metal with zero gap semiconductor behavior (Dresselhaus, Dresselhaus and Saito 2001).

Given that bonding is trigonal planar within the graphene plane and these graphene planes are held together by weak van der Waals forces in between graphene planes, the graphite crystal is anisotropic.

Crystallographically, graphite has a unit cell that resembles a unit cell belonging to a hexagonal close-packed (HCP) material. Graphite has a unit cell with four atoms and the unit cell has an a-axis dimension of 2.46Å and a c-axis dimension of 6.71Å. Figure 4 shows graphite's unit cell.

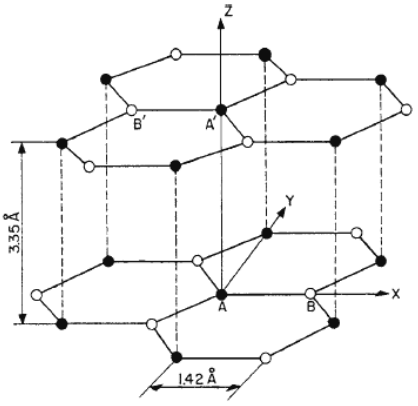

Figure 4: The crystal structure of graphite. The dimensions shown here are the in-plane bond lengths (Chung 2002).

Graphite has two different stacking sequences, alpha (hexagonal) and beta (rhombohedral). Alpha stacking is the most common and the thermodynamically stable stacking sequence. Beta stacking is less common and thermodynamically unstable. Beta stacking has three layers designated as A, B, and C that are stacked in an ABCABC sequence. Beta stacking is considered a stacking fault of alpha stacking. Alpha stacking has two layers denoted as A and B that are in an ABABAB stacking sequence. Some

crystallographic defects of graphite include screw and edge shear dislocations and nonparallel graphene planes (known as disinclination). Graphite that has no evidence of long-range order is known as turbostratic graphite. Upon heating, graphite increases its order of crystallinity.

Graphite properties are heavily dependent on the method of manufacture as well as the raw materials involved in graphite's manufacture. The precursor materials are split into four categories: fillers, binders, impregnants, and additives. The filler of choice in graphite manufacturing is a petroleum coke. Petroleum coke is a byproduct of the petroleum industry. Petroleum coke is porous and is a nearly pure carbon solid at room temperature. In addition, petroleum coke is used given that it is easily graphitized between 2800-3000°C (Eatherly and Piper 1962). Petroleum coke is boiled at pressure to 430°C then is calcined at 1300°C to remove any residual hydrogen to yield calcined coke (Pierson 1993).

The next precursor material is a binder, which is most commonly coal-tar pitch. There are several requirements for a binder, those requirements being that it is thermoplastic (solid at room temperature and fluid at elevated temperatures) given that this facilitates thorough mixing of the filler and binder. It is also required that the binder has a high carbon content and that the majority of this carbon be deposited as a bonding coke by some process and that the specific gravity is as high as possible so there are the highest number of atoms around the filler coke as possible (Eatherly and Piper 1962).

When it comes to production, the first stage in the manufacturing process is to grind the binder and the calcined filler into "flour", the size of which can vary from very small

to large (1 micron to 1.25 centimeters) (Pierson 1993). This stage is known as milling and sizing. The next stage is to coat each filler particle with binder, which is conducted at elevated temperatures, usually 160ºC to 170ºC (Pierson 1993). Next, a forming process is selected for the graphite, which can be vibramolded, extruded, or isostatically pressed. Extrusion is favored for producing parts having a constant cross section and is the most common method. Isostatic pressing is favored for material requiring great uniformity. The forming process yields a green artifact, which is ready for carbonization.

Carbonization takes place at 1000°C and may last from a few days to several weeks. This process causes the binder to soften and causes volatiles to be released. In addition, material shrinkage and material hardening occurs. The carbonization stage yields a baked artifact, which has high porosity and therefore requires densification through impregnation.

Impregnants are commonly coal-tar pitch or a polymer such as phenolic (Pierson 1993). After initial impregnation, the baked artifact is then rebaked. The green form is then impregnated again. Impregnation occurs multiple times until the green form is fully dense. Then the impregnated and baked artifact is ready for graphitization, which increases the material's resistance to thermal shock and chemical attack as well as increases the thermal and electrical conductivities. The graphitization stage is generally shorter than the baking/carbonization stage. Additional stages of manufacturing include purification. Purification is conducted on graphites requiring high degrees of purity and involves heat treatment in a halogen atmosphere, which removes metals and boron via volatile halide formation, which then diffuses out of the graphite (Pierson 1993). The

final graphite product's properties are heavily dependent on the characteristics of the filler-binder mixture. A schematic of the polygranular graphite structure is shown in Figure 5. Some graphite micrographs are shown in Figure 6.

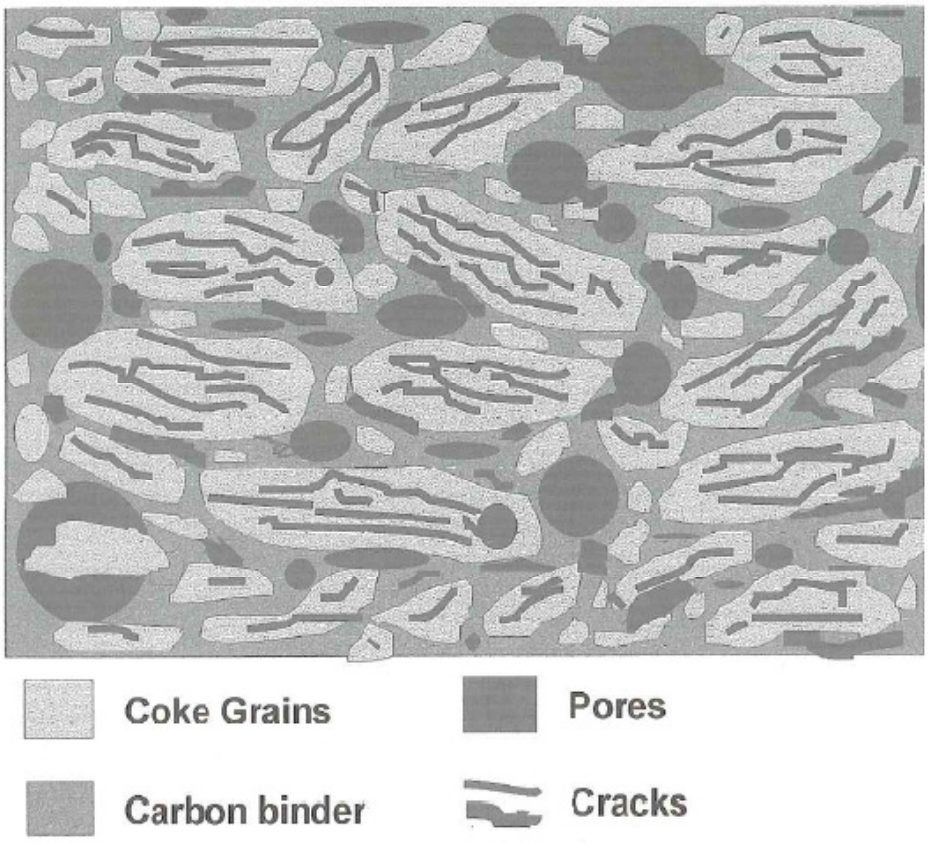

Figure 5: Polygranular graphite structure showing that there are pores and cracks in the coke grains as well as pores in the binder phase (Rand 2001).

Figure 6: Graphite micrographs with pores, coke/filler, and the binder phase denoted (W. Windes 2010).

A diagram of the graphite manufacturing processes is shown in Figure 7.

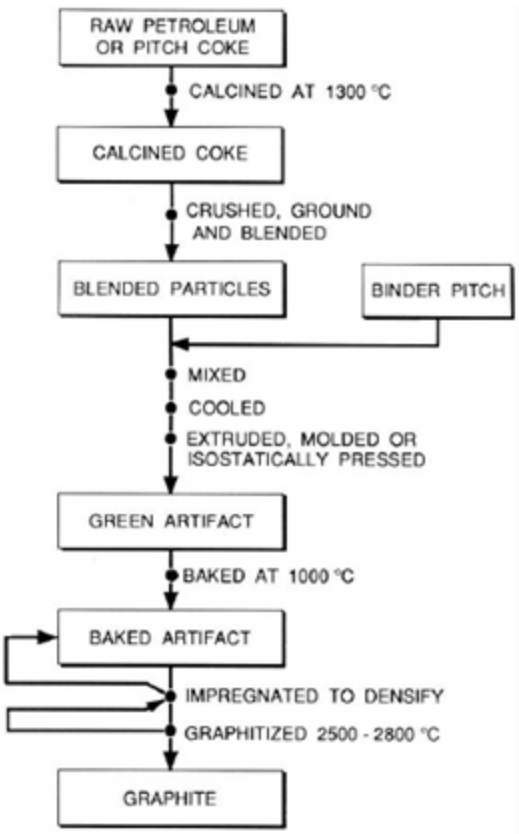

Figure 7: A typical graphite manufacturing process (Windes, Burchell and Bratton 2007).

Graphite is more thermodynamically stable than diamond at room temperature (refer to the carbon phase diagram in Figure 8) and is also stable at elevated temperatures as long as it is maintained in a non-oxidizing environment. Graphite also has high thermal conductivity and a low coefficient of thermal expansion as well as a high adsorption of gases and resistance to thermal shock. Graphite is relatively easy to machine as well.

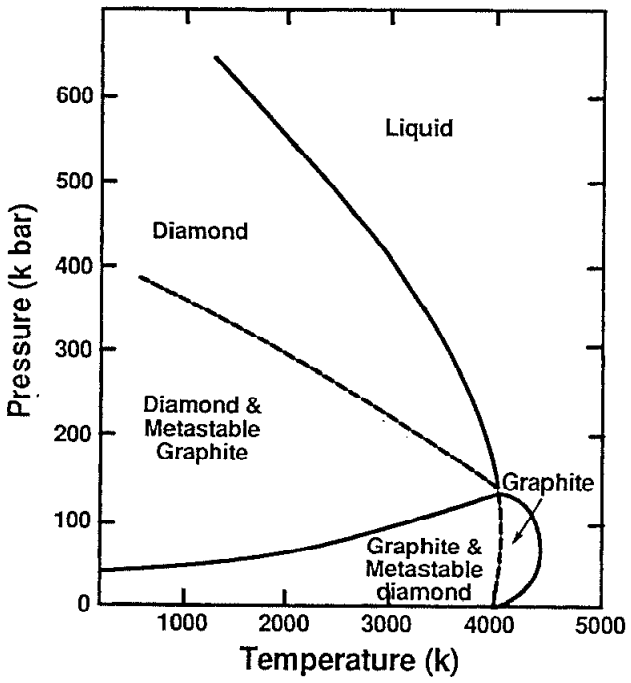

Figure 8: Carbon phase diagram (Pierson 1993).

Graphite is unique in its refractory properties in that it has the second lowest density of all refractory materials and it has one of the highest melting points of all materials. In addition, graphite does not melt at ambient pressure (1 atm) but rather it requires 100 atm and 4200ºK to melt (Pierson 1993). Graphite requires an immense amount of energy to vaporize, which is why it is used in many aerospace applications such as nose cones and rocket nozzles. Other applications of graphite include heating elements in furnaces, high temperature refractories, arc welding electrodes, chemical reactor vessels, electrical contacts, metallurgical crucibles, brushes and resistors, air purification devices, and battery electrodes (Pierson 1993). The application of graphite that is pertinent to this research is as a component (be it structural or otherwise) in a nuclear reactor.

2.2 Nuclear Graphite

2.2.1 Introduction to Nuclear Graphite

Non-specialty graphite would not be sufficient in a nuclear application for many reasons ranging from the existence of impurities leading to modified nuclear properties, to an insufficient degree of graphitization and isotropy. A special grade of graphite known as nuclear graphite is manufactured just for this purpose. Nuclear graphite requires a high degree of isotropy given that dimensional changes that occur during irradiation must be as predictable as possible. A high degree of purity is required of nuclear graphites given that any presence of an impurity, especially boron, will affect graphite's behavior as a moderator in a nuclear reactor by increasing graphite's neutron absorption cross section. The existence of impurities may also lead to the development of intercalation compounds and to the formation of unwanted activation products during irradiation. Other elements that are undesirable in graphite include hydrogen, nitrogen, chlorine, titanium, vanadium, and rare earths—these all have absorption cross sections that can increase graphite's absorption cross section (Nichols and Woodruff 1962).

Nuclear graphite must be highly crystalline, but not to the degree of highly oriented pyrolytic graphite (HOPG), which has the highest order of crystallinity of any manufactured graphites. When graphite undergoes irradiation, it experiences dimensional changes caused by ballistically generated interstitial defects mobilizing and finding areas usually between the graphene planes to settle. Nuclear graphite irradiation behavior is easier to model when the nuclear graphite is highly crystalline and isotropic.

Graphite exhibits certain properties that make it a suitable material for use as a neutron moderator. The requirements of any moderator include that it must slow fast neutrons to thermal speeds, and have a small neutron absorption cross section. Any slowing of neutrons happens because of an energy loss due to elastic collisions between moderator nuclei and neutrons. The nuclear performance of a moderator is a combination of its ability to slow neutrons to thermal speeds with its ability to capture neutrons. A good moderator will have a high slowing down power and low absorption ability (T. D. Burchell 2001). Nuclear graphite has a small neutron absorption cross section and a high neutron scatter cross section and is an effective moderator.

Graphite is also used in nuclear reactors as a reflector and as a structural component. The purpose of the reflector is to reflect neutrons back into the core so that they may again take part in fission in order to sustain the chain reaction that keeps the reactor powered.

2.2.2 Graphite Irradiation Behavior

The simple structure of graphite vastly simplifies the irradiation damage mechanism (Kelly 1981). Upon neutron irradiation a neutron will knock carbon atoms from the basal plane and cause the formation of a vacancy, as shown in Figure 9.

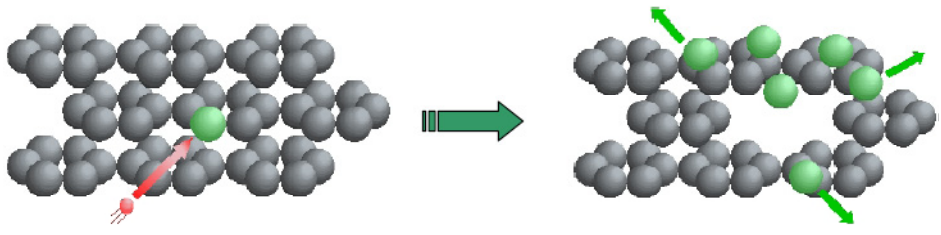

Figure 9: Diagram of graphite neutron damage (Windes, Burchell and Bratton 2007).

The atom that is knocked out, called the primary knock-on atom, may knock out other atoms from the basal plane in a cascade effect. These other atoms that are knocked out are called secondary knock-on atoms. The two factors affecting the extent of damage in graphite during irradiation are the number of primary knock-on atoms and the energy of the primary knock-on atom, which is dependent on the energy of the colliding neutron (De Halas 1962).

These displaced atoms resulting from a collision with a primary knock-on atom may resettle in existing vacancies along the basal plane, or they may more commonly settle in the lower energy area between the graphene planes, which is shown in Figure 10.

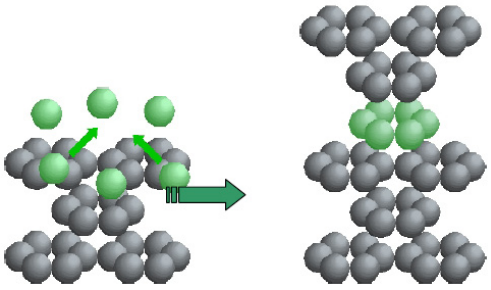

Figure 10: Diagram of displaced carbon atoms settling between basal planes during neutron damage (Windes, Burchell and Bratton 2007).

Clusters of displaced atoms may also coalesce and form a dislocation loop that is the start of another graphene plane. These new planes grow and form fully sized planes. This damage mechanism causes a net expansion in the c-axis (perpendicular to the basal plane) and a net contraction along the a-axis (along the graphene plane). In the beginning of neutron irradiation, net volume shrinkage of the graphite occurs given the existence of thermal shrinkage cracks that accommodate the c-axis expansion (Burchell and Snead 2007). As neutron irradiation continues, the c-axis continues to expand and pore generation begins. This point where the net volume shrinkage changes to expansion is

known as “turnaround”. After this turnaround, pore generation and expansion will continue until internal stresses within the graphite microstructure are large enough to propagate cracks.

The mechanical properties of graphite change drastically under irradiation (Kelly 1981). Neutron irradiation alters the pore structure of graphite and when tested in tension, graphite preferably fails at the site of a flaw or a pore.

2.3 Mechanical Testing of Graphite

2.3.1 Mechanical Properties of Nuclear Graphite

The specific properties that are needed to demonstrate that graphite meets requirements for the NGNP, which tensile testing can provide, include the ultimate tensile strength, and strain-to-failure. The mechanical properties of nuclear graphite need to be characterized especially post-irradiation in order to have an understanding of how the material changes during irradiation, which will define a working envelope for the graphite to be used in a reactor. In addition, since the graphite is being used as a structural element, knowledge of the mechanical properties is important.

Some basic definitions used in graphite mechanical testing are those for ultimate tensile strength, strain, and brittle. The ultimate tensile strength is the highest strength attained in tension before the material fails. The strain is the change in length per unit length (so it is a dimensionless quantity) and represents how much the material deforms while it is being stressed. Brittle means that a material does not deform much plastically before failing. Brittle failures are often abrupt.

2.3.2 Sample Size and Mechanical Testing

According to Annex 4 of the ASTM Standard C 781-08, the recommended small specimen diameter is 6.5 millimeters (mm) and the recommended height-to-diameter ratio is 4. The AGC-1 samples have a height-to-diameter ratio of 2 given that they are

12.70 mm in diameter and 25.40 mm high; therefore, any testing of them would be a deviation from the ASTM standard.

The grain structure of the graphite heavily influences any mechanical properties. The grain structure will depend on the method of manufacture as well as the precursor materials used during manufacturing. There are graphites with fine grains such as Toyo Tanso's IG-110 and some medium-grained graphites such as SGL's NBG-18.

In fine-grained graphite, the number of grains for a given diameter is not problematic since there are more than enough grains to represent bulk properties at such a small diameter. In a medium-grained graphite such as NBG-18, when a diameter is small (such as 12.70 mm), that may only be seven or eight grains (NBG-18 has a maximum grain size of 1.6 mm), which may not be representative of bulk properties. According to ASTM Standard C 749-08, the gauge diameter of a specimen should not be reduced to less than three to five times the maximum grain size of the material otherwise the results may be erratic.

It is unclear whether or not the ASTM standard required small sample diameter of 6.5 mm would be adequate for NBG-18 given that 6.5 mm is approximately equal to 4 grains. The topic of this thesis is whether or not a certain diameter is adequate in representing the bulk properties of a medium-grained graphite.

2.3.3 Previous Studies with Small Samples

Previous studies on small samples include a study from Oak Ridge National Laboratory, which constituted the development of glue-up small sample testing (Burchell,

et al. 2009). The study was aimed at finding a way to mechanically test the AGC-1 samples that were of a set diameter that is smaller than what the ASTM standard calls for. The study involved gluing the samples in a manner similar to the one used in this study but using different alignment media and adhesives.

A method of gluing the sample for tensile testing was previously published by A.L. Pitner where it was reported that after several attempts to break the sample, the glue would always fail before the graphite sample (Pitner 1971).

2.4 An Overview of Graphite Fracture Mechanics

Graphite is a brittle material given that it undergoes no plastic deformation and strain before it fractures in tension. Any strain is not due to actual plasticity but rather the formation of cracks. The fracture surface of graphite is also characterized as being a classic brittle fracture given the flat faces of the fracture surfaces and the lack of any ductile characteristics such as a cup and cone fracture. In Figure 11, a comparison between brittle and ductile fractures is given and in Figure 12, an image of a broken specimen from this study is shown to demonstrate its correspondence to a brittle fracture.

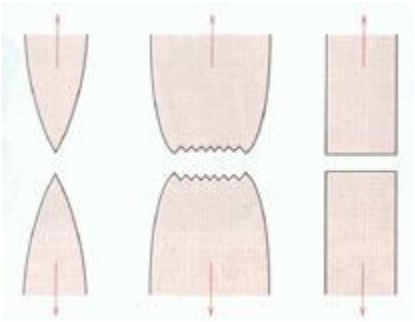

Figure 11: Very ductile (left), ductile (center), and brittle fractures (right) (William D. Callister 1994).

Figure 12: A broken graphite small sample from this study, demonstrating brittle fracture behavior.

Brittle fractures expend less energy than ductile fractures and are characterized by rapid crack propagation and very little or no plastic deformation (Gross 1996).

Graphite fractures in tension in Mode I [Opening Mode] fracture by cracking. A diagram of Mode I fracture is shown in Figure 13.

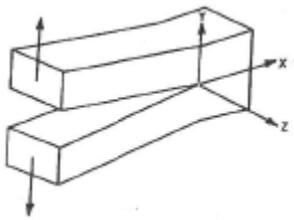

Figure 13: Diagram of Mode I or Opening Mode fracture (Barson and Rolfe 1999).

There are three further modes of brittle fracture modes developed by Ghandi and Ashby. These fracture classifications are also known as Modes I-III although these modes differ from Opening Mode [Mode I], In-Plane Shear [Mode II] and Out-of-Plane Shear [Mode III]. Graphite breaks in Mode I fracture in the Ghandi-Ashby classification system given that Mode I fracture stems from preexisting flaws at low stresses (Gross 1996). Graphite is a very porous material; therefore, there are many pores with their associated stress concentrations that can serve as the site of crack formation and propagation.

The progression of brittle fracture in graphite begins with a pre-existing flaw in the graphite. This flaw could be a pore or another feature developed during manufacturing or during operation. The flaw then propagates in a stable mode due to loading with the initial growth rate being small but accelerating with time. The flaw/crack then reaches a critical size, fracturing very quickly at speeds close to the speed of sound (Antolovich and Antolovich 1996).

3. Experimental Procedure

The focus of this thesis is to determine whether there is a correlation between the failure tensile stress and the number of grains across the diameter of a small specimen. This requires the tensile testing of these small samples; however small samples cannot be machined into traditional ASTM standard tensile test samples. ASTM standard C 781-08 has a method outlined for gluing a small graphite specimen to threaded inserts to make the sample mimic an ASTM standard tensile test sample. Shown in Figure 14 are the components making up the small sample tensile specimen. To form a small sample tensile specimen, the graphite specimen is adhered to threaded aluminum inserts which are shown immediately on either side of the graphite specimen in the center in Figure 14. After the graphite is bonded to the aluminum inserts, the aluminum threaded ends are screwed into stainless steel grip ends, which are shown next to the aluminum threaded inserts in Figure 14. In Figure 15, a small sample tensile specimen is displayed with an ASTM standard tensile specimen. The small sample tensile specimen has the same style of grip ends as the ASTM standard specimen; therefore it may be tested using the same load train that is prescribed for use with the ASTM test method.

Figure 14: The components making up the glued-end tensile test specimen (top) and the assembled glued-end specimen (bottom) (Carroll, Swank and Windes 2009).

Figure 15: A standard graphite tensile test specimen (top) and a glued-end tensile test specimen (bottom) (Burchell, et al. 2009).

A consideration in the assembly process of small sample tensile specimens involved the graphite specimen's alignment with the aluminum threaded inserts and the grip ends. Specimen alignment is crucial to ensure there is no bending moment when the sample is tensile tested. A special alignment jig was fabricated and is shown aligning the graphite specimen to its threaded inserts and grip ends in Figure 16. This alignment jig was used to keep all of the pieces of the small sample tensile specimens in alignment while the adhesive cured.

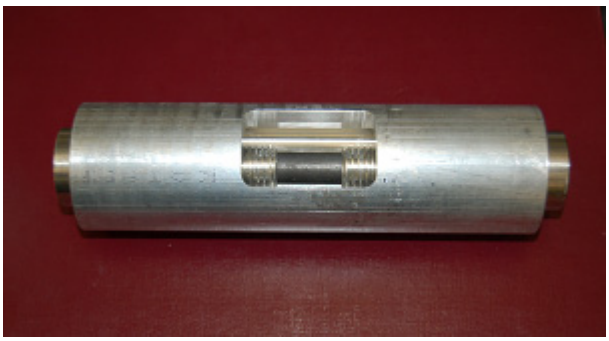

Figure 16: The jig used to ensure proper alignment of the graphite small sample.

An additional consideration in the assembly process involved the thickness of the glue layer applied to the graphite specimen. Uniformity of glue thickness is important to the alignment of the small sample tensile specimen and was achieved by placing two Nichrome wires between the graphite specimen and the aluminum threaded insert on each side for a total of four Nichrome wires in the small sample tensile specimen assembly.

An extensometer was attached to the graphite specimen to measure strain behavior and is shown attached to a graphite small sample tensile specimen in Figure 17. The extensometer is the device that is connected using rubber bands to the graphite small sample tensile specimen. The extensometer knife edges could potentially slip on the graphite surface therefore two small patches of quick curing epoxy (different from the adhesive used in this study) were applied to the area where the extensometer knife edges would contact the sample. These small patches of epoxy served to properly seat the extensometer knife edges without reinforcing the strength of the graphite.

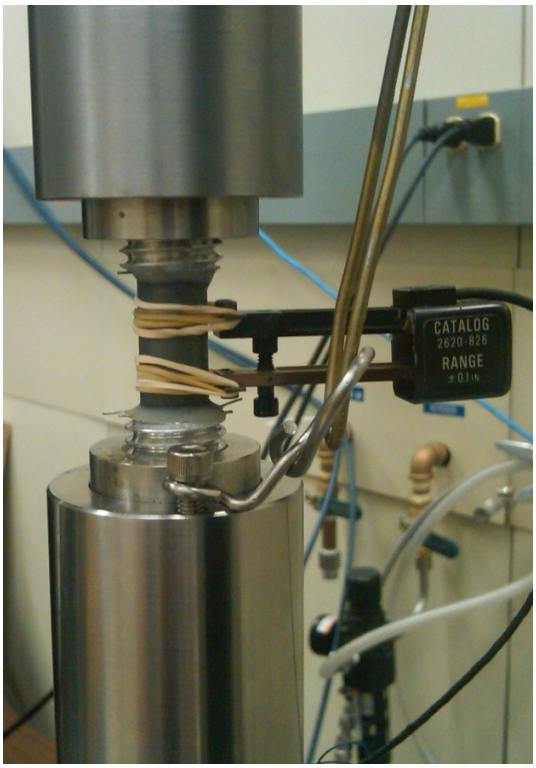

Figure 17: The graphite sample in the test fixtures with the extensometer attached.

All tension tests were conducted on an Instron 4505 Universal Test System load frame (serial number H2405). The load cell was an Instron static 5 kilonewton (kN) capacity load cell (serial number 142). Values obtained from the load cell have an uncertainty of 0.5% of the reading or 0.25% of the full scale measurement range,

whichever was larger. The extensometer was an Instron dynamic ± 0.1 inch range extensometer (model number of 2620-826, serial number of 11237). The extensometer had a resolution of 5×10^{-6} inches. The extensometer was calibrated daily using a calibrated Epsilon calibration stand (serial number 3778). Initial specimen dimensions were taken using a Nikon profile projector fitted with two calibrated Mitutoyo micrometers with resolutions of 1 micron ± 3 microns over their full 50-mm range of travel. Post-test measurements were taken with calibrated SPI calipers (serial number 9001633).

The billet from which the graphite samples were machined was manufactured by SGL and was grade NBG-18. The original billet size was 1950mm X 540 mm X 500 mm and had a maximum grain size of 1.6 mm.

3.1 Adhesives

The focus of this module of the experiment was to find a suitable adhesive to use in assembling the glued end tensile specimens for the study. While the ASTM standard (C 781) modification (of C 749) allows for gluing small graphite samples to special fixtures for testing, no adhesive is defined for the application. A traditional epoxy is generally not suitable for small sample graphite specimen adhesion because most commercial epoxies are unable to bond to graphite and do not have sufficient strength. An adhesive suitable for this application must bind the graphite to the aluminum and have a greater ultimate tensile strength than the graphite.

Additional favorable, but optional, features of a suitable adhesive include a short cure time, ease of use (i.e. single-component versus multi-component), reasonable cost, and ease of disposal. Some epoxies are considered hazardous waste and therefore cannot be dumped in a landfill.

The technical data sheets of several epoxies and adhesives and thermoset glues have values for lap shear strength, cure time, use and disposal instructions, and associated hazards. These values serve as the first screening for the suitability of an adhesive. After selected adhesives are ordered and received, they are used in making glued-end tensile specimens, which will test both the adhesive's ability to bind the graphite and the aluminum threaded end and the adhesive's tensile strength.

The adhesive used in the preliminary ORNL study was Lord 310 A/B two-part epoxy. This adhesive has some shortcomings in that it is considered hazardous waste, it is more

expensive than other options, and 24 hours are required for curing. For these reasons, study authors recommended evaluation of alternative adhesives in a future study.

Six adhesives, listed in Table 1, were chosen for testing. Table 1 also lists lap shear strength values provided by the manufacturer of each adhesive.

Table 1: Adhesive lap-shear strengths as reported by the manufacturer.

	Maximum Lap Shear Strength (MPa)
Hardman Double/Bubble Epoxy	20.68
Lord 310 A/B Epoxy	19.24
CLS 9420 Structural Adhesive	14.48
SystemThree GelMagic Epoxy	19.31
Devcon 5 Minute Epoxy	13.10
Krazy Glue Cyanoacrylate Adhesive	13.79

Each candidate adhesive was used to prepare graphite test samples and was evaluated with respect to strength of the bond between graphite and aluminum components. Adhesives were expected to maintain the bond between components to stresses greater than 20 MPa, approximately the stress at which graphite fails in tension.

3.2 Validation of Glued Sample Testing

The purpose of this module was to demonstrate that small, glued end tensile specimens and full-sized, non-glued tensile specimens would perform similarly in tests of ultimate tensile strength. Thirty-eight small samples were made and tensile tested using all of the same equipment—same load frame, test fixtures, extensometer (that was calibrated each day before the tests) with the same batch of adhesive. Forty full size samples were tensile tested using the same testing conditions. A summary of tensile tests used for the validation of glued sample testing is shown in Table 2.

Table 2: Graphite samples tested for comparison of ultimate tensile strength and strain-to-failure.

	ASTM Standard Tensile Test Samples	**Small Samples**
Number	40	38
Diameter	5/8 inch	½ inch

There is an unavoidable stress concentration at the ends of the samples because a significant change in the cross-sectional area of the sample results in heightened stresses in that area. The drastic change in cross sectional area of the sample occurs where the holes are drilled in the ends of the graphite specimen to accommodate the pins on the aluminum threaded ends for graphite specimen alignment purposes. A diagram of the graphite specimens used in this experiment is shown in Figure 18.

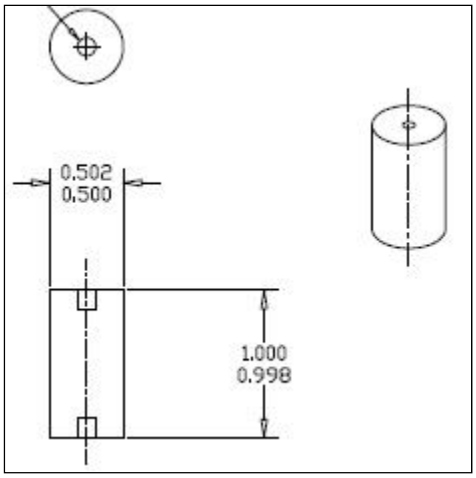

Figure 18: Geometry and dimensions (inches) of graphite samples used in this experiment.

Another area of stress concentration is at the glue joint between the graphite specimen and the aluminum threaded end.

Because of this stress concentration, the graphite sample will more likely break near the ends of the sample (near the grip ends) than in the gauge.

3.3 Sample Diameter Reduction Studies

The objective of this module was to determine whether there was a correlation between the failure tensile stress and the diameter of the glued end tensile specimen.

Because of limited irradiation space in materials test reactors, only small irradiated samples will be available for the NGNP qualification testing. Therefore, it is important for the NGNP program to demonstrate that graphite samples with diameters smaller than ASTM standard tensile test samples are viable for mechanical testing.

After the graphite sample dimensions were measured and documented, adhesive was applied to bond the graphite to the aluminum threaded ends. The adhesive was cured in an oven at 150ºC. After curing and cooling, the sample was machined down to a reduced diameter with a fillet on each end (see Figure 19).

Figure 19: Reduction of diameter of the specimens. The original specimen geometry (diameter of 12.70 mm) is on the left. (Carroll, Swank and Windes 2009).

The original specimen geometry, with diameter of 12.70 mm, is the left-most sample in Figure 19. The center specimen in the figure denotes a specimen mechanically reduced to 10.00 mm in diameter and the specimen on the right represents a mechanically reduced specimen of 8.00 mm in diameter. Fillets were machined into the specimens so as to limit

the influence of the stress concentration from the glued end as well as to promote the sample breaking in the gauge section.

4. Results

4.1 Adhesives

The objective of the adhesives module of the experiment was to find a suitable adhesive that would bond the graphite to its aluminum threaded ends to strengths around 20 MPa. Six adhesives were separately used to glue the graphite specimens to their aluminum threaded ends. When the adhesive was dry, bond strength was tested by placing the glued unit in tension until the sample or the adhesive failed.

Although an adhesive might have a high lap shear strength that does not necessarily imply that it will effectively bond the graphite to the aluminum end threads or load to the requisite tensile strength. Every adhesive was tested for bonding the parts of the tensile specimen.

Most of the adhesives debonded when subjected to stresses between 3 MPa and 7 MPa. Debonding did not occur with two of the adhesives, namely the Lord 310 A/B two-part epoxy (which was known to be an effective adhesive for this application) and the CLS 9420 structural adhesive.

The CLS 9420 was ultimately selected as the adhesive for all samples tested in this study. It has a significantly shorter cure time than the Lord 310 Epoxy (1 hour versus 24 hours) and it is a single component structural adhesive, eliminating failure due to incorrect mixing of resin and hardener (for a two-part epoxy). In addition, CLS 9420 is not considered hazardous waste (whereas the Lord 310 A/B epoxy is hazardous waste and must be disposed of accordingly), and is less expensive.

After choosing the CLS 9420 adhesive, a set of small graphite samples was glued and tensile tested to confirm the adhesive did not fail before the graphite. This set of samples was denoted the CLS series of tests, numbered 1-6. The stress-strain curves for the CLS series of graphite specimens is given in Figure 20. Each sample broke between 19 and 23 MPa. In this set of tests, the graphite specimen failed whereas the adhesive remained intact. Use of this adhesive for graphite small sample gluing was further validated by adequate performance in all testing performed as part of this research. CLS sample number 2 was removed from the data set because the equipment measuring the strain malfunctioned during the test.

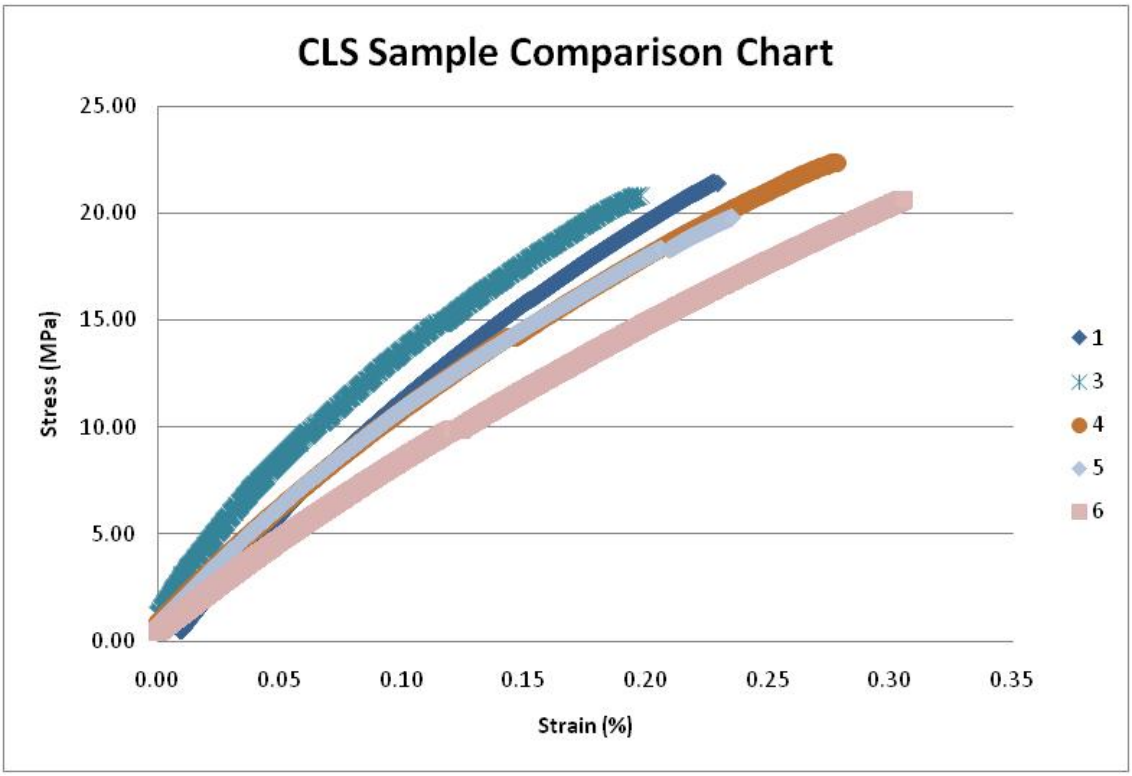

Figure 20: Stress-strain curves for CLS adhesive test samples.

4.2 Small Sample Validation

4.2.1 Small Samples

The goal of the first part of the small samples validation was testing repeatability. These samples are denoted as Statistical and Quality, (SQ). Thirty-eight samples were assembled and tested in tension, yielding the results plotted in Figure 21. The standard deviations for the stress and strain were 1.559 MPa and 0.07384, respectively. The results are summarized in Table 3.

Table 3: SQ sample averages and standard deviations for stress and strain.

	Average	**Standard Deviation**
Stress (MPa)	19.78	1.559
Strain	0.2579	0.07384

Graphite is a brittle material; therefore, the average strains to failure are very small, averaging around 0.25%. The average failure strengths are about 20 MPa for these smaller samples.

In Figure 21, the stress-strain curves for all of the SQ samples are shown.

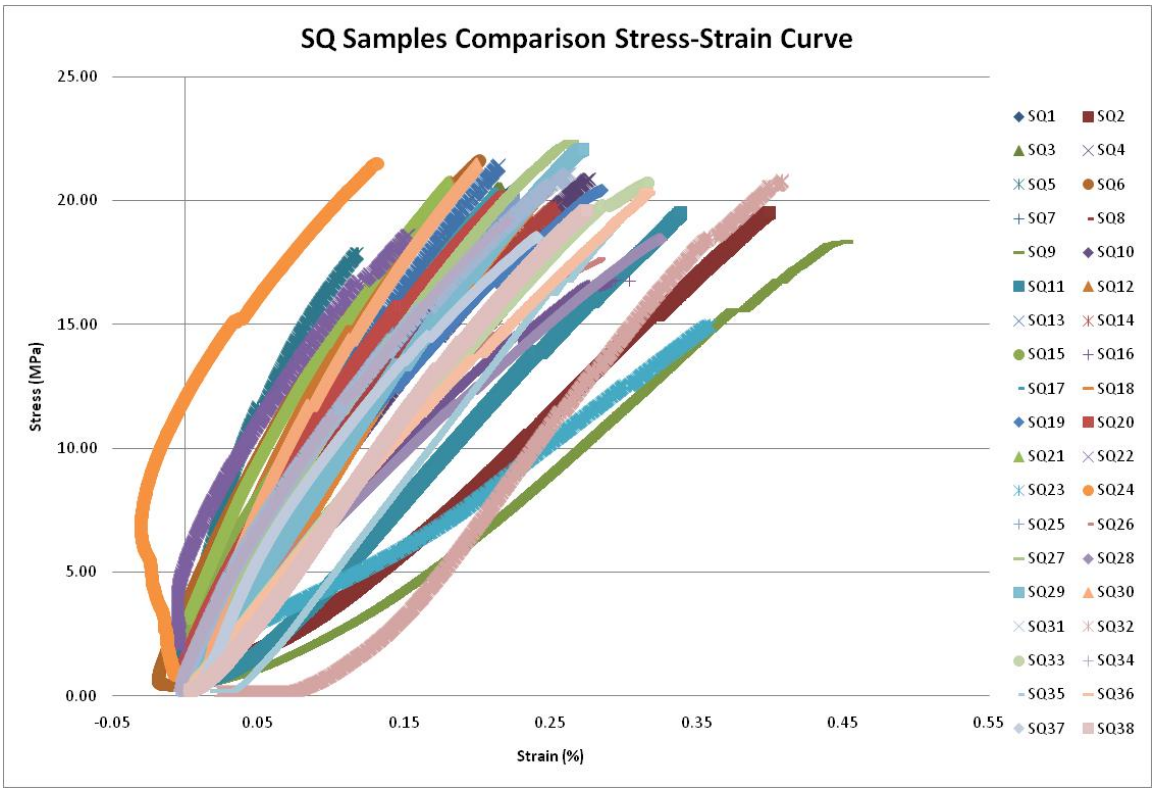

Figure 21: Comparison chart of the SQ small sample validation studies.

It is apparent in Figure 21 that an initial, significant negative strain occurred in several graphite samples (most notably SQ24), before a shift to positive strain. This phenomenon likely is due to a bending moment in the test fixtures or to a relaxation in the graphite when it is slightly preloaded in the test fixtures. Some of the positive strain jumps may be attributed to sample cracking.

As can be seen in Figure 21, the stress-strain curves are the same basic shape and fail in the same range of stress (between 18 and 23 MPa). Based on these tests it can be concluded that the results are repeatable.

4.2.2 ASTM Standard Samples

The goal of the second part of the small samples validation was to compare the results of small sample testing with those for full size ASTM standard samples. Because qualification of graphite for NGNP requires testing of small, irradiated samples, it is crucial to demonstrate that small sample tensile specimens behave as full size ASTM standard samples. If the small sample tensile specimens do not perform as the ASTM standard samples do, tensile testing of the small, irradiated graphite samples will not yield useful data.

Forty full size ASTM Standard quality-level samples were tensile tested for comparison to the small samples. The samples are denoted as Full Size (FS). The results are summarized in Table 4.

Table 4: FS sample averages and standard deviations for stress and strain[a].

	Average	**Standard Deviation**
Stress (MPa)	19.09	1.693
Strain	0.2603	0.02619

[a] The graphite data for the Full Size (FS) samples are from the NGNP graphite baseline activity and were conducted by Dr. Mark Carroll.

The resulting data are shown in Figure 22 and the stress-strain curves are plotted in Figure 23.

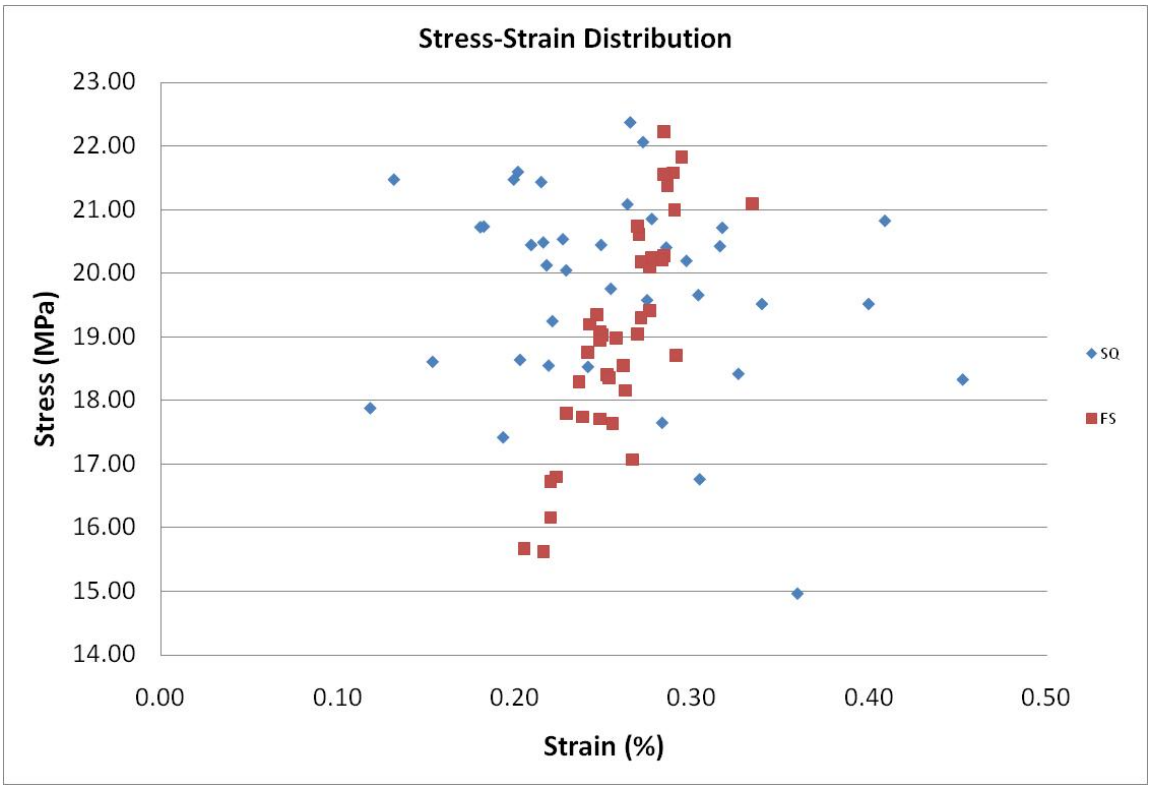

Figure 22: Stress and strain values at graphite sample failure for the FS (full size) and SQ (Statistical and Quality) sample sets.

In Figure 22, the stress and strain values are plotted for two sets of samples. Results of testing the full size (FS) samples fall within a narrower range of strain values than the SQ sample results; however, the results indicate that both the FS samples and the SQ samples break in the same range of stresses.

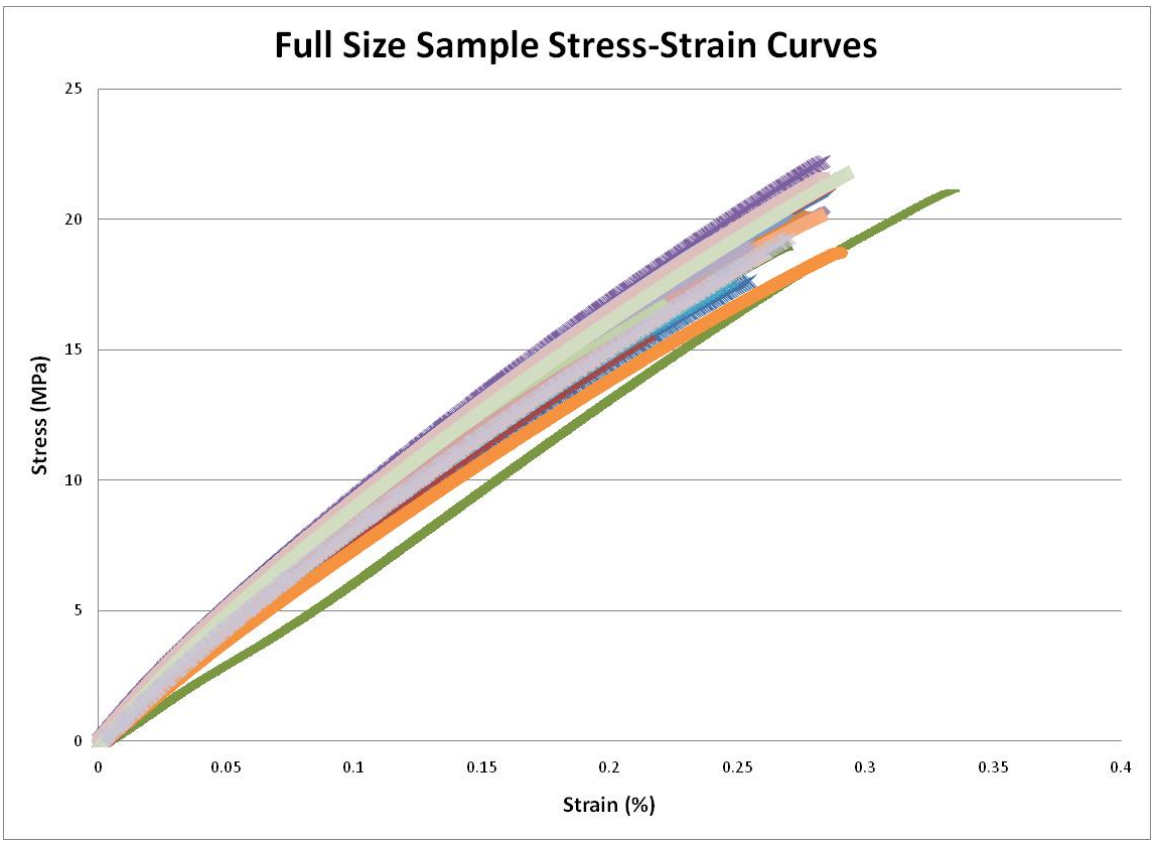

Figure 23: Stress-strain curves for 40 full size samples.

Comparison of Figure 21 and Figure 23 reveals a significantly tighter distribution for stress-strain curves of the full size samples than for the small SQ samples. Test results for the small samples may have greater scatter due to sample origin in a billet of graphite known to have less consistency than the billet from which the full size samples were obtained (W. Windes 2010).

Data scatter on the plots in Figure 22 and Figure 23 is further indication of the brittle, porous and flawed nature of graphite. Brittle fracture in graphite qualifies as Ghandi-Ashby Mode I fracture, meaning failure occurs at low stresses due to a preexisting flaw. Because graphite consists of coke surrounded by fillers, binders and impregnants, there are many potential sites for flaws and associated stress concentrations. These stress

concentrations will be in the vicinity of pores, cracks and areas of nonhomogeneity, which constitute the pre-existing flaws classified in the Ghandi-Ashby system. Because graphite macro-structure varies from sample to sample and within a specific sample, there may be thousands of areas of stress concentration, any one of them a potential crack propagation site. A stress concentration may be large or small and, therefore, instigation and propagation of cracks will occur at different rates. Such variability leads to data scatter. The results of tensile testing for several samples indicate an increase in strain at some point in their stress-strain curves, which is due to the extensometer detecting a crack. Further study of this strain phenomenon is outside the scope of this thesis.

The failure stresses of the SQ and FS samples are very similar to each other—the SQ samples had an average stress of 19.78 MPa with a standard deviation of 1.559 MPa, and the FS samples had an average stress of 19.09 MPa with a standard deviation of 1.693 MPa. Test results for both sample sets are summarized and compared in Table 5.

Table 5: Summary comparison of SQ and FS sample average stresses, strains and standard deviations.

	Average Stress (MPa)	**Average Strain**	**Stress Standard Deviation (MPa)**	**Strain Standard Deviation**
SQ Samples	19.78	0.2579	1.559	0.07384
FS Samples	19.09	0.2603	1.693	0.02619

4.3 Reduced-Diameter Samples

The goal of the reduced-diameter samples module of the experiment was to assess whether or not there was an effect on tensile strength when the sample diameter was reduced. The results of the reduced-diameter sample tests and their corresponding diameters are given in Figure 24. Samples that have been reduced to 10 mm in diameter are denoted as Reduced Diameter 10 mm (RD10) samples. Samples that have been reduced to 8 mm in diameter are denoted as Reduced Diameter 8 mm (RD8) samples. The results are summarized in Table 6.

Table 6: Averages and standard deviations of the stress and strain test results for the Full-Size samples, the Statistical and Quality samples, the Reduced-Diameter 10 mm samples and the Reduced-Diameter 8 mm samples.

	Average Stress (MPa)	**Average Strain**	**Stress Std. Dev. (MPa)**	**Strain Std. Dev.**
Full Size (FS)	19.09	0.260	1.69	0.026
Statistical and Quality (SQ)	19.78	0.258	1.56	0.074
Reduced Diameter 10 mm (RD10)	17.26	0.289	2.28	0.15
Reduced Diameter 8 mm (RD8)	16.86	0.285	1.98	0.084

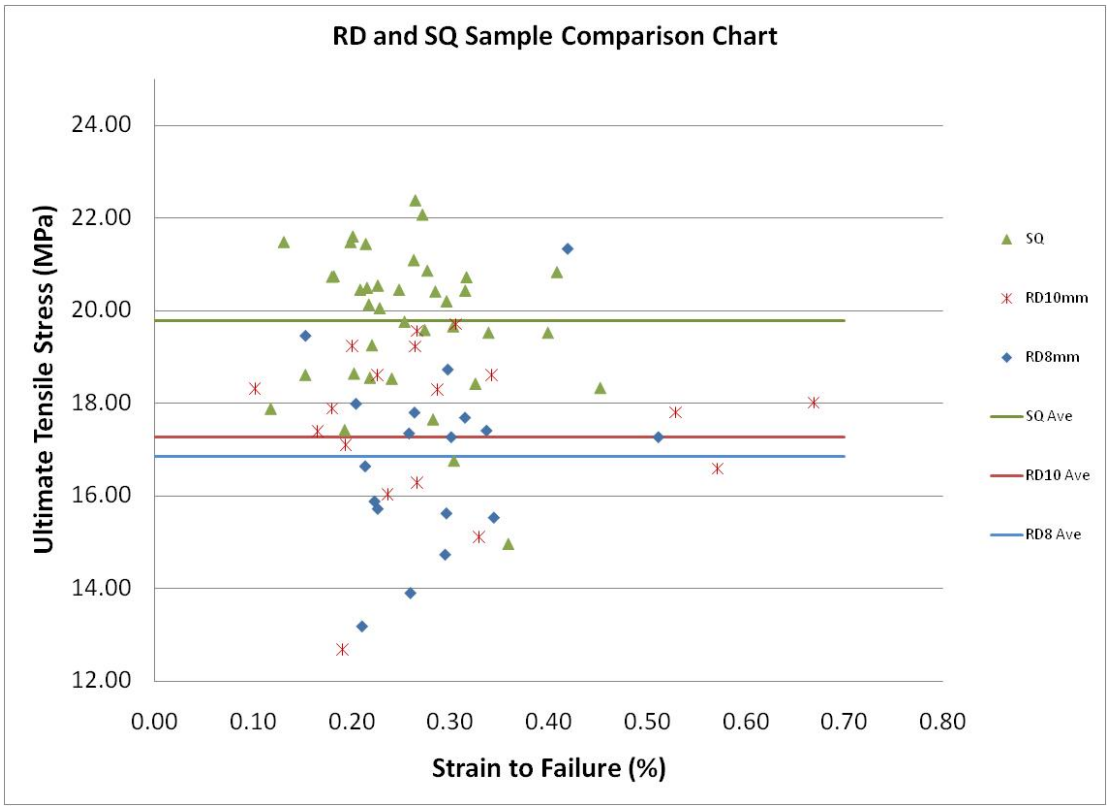

Figure 24: Comparison of tensile test performance for 8-mm (RD8), 10-mm (RD10), and 12.7-mm (SQ) diameter samples.

Figure 24 shows three sets of data along with three lines representing the average values for the three sets of data. The top line corresponds to the average failure tensile stress of the original (SQ) small samples (which are denoted by triangles), which have diameters of 12.70 millimeters (mm). Similarly, the middle line in the figure corresponds to the 10.00-mm (RD10) diameter samples (which are denoted by "x" shapes) and the bottom line corresponds to the 8.00-mm (RD8) samples (which are denoted by diamonds).

The SQ samples are grouped together at an overall higher tensile stress than both the RD10 samples and the RD8 samples. This is demonstrated by the average line for the SQ samples (the top line) being above the other two lines representing the reduced diameter samples. The RD10 samples are grouped together at a slightly higher stress than the RD8

samples, again shown by the average line for the RD10 samples (the middle line) having a higher value of tensile stress than the average line for the RD8 samples (the bottom line).

As can be seen in Figure 24, there is in fact a reduction in stress required to break the sample when the sample diameter is reduced. The original small samples with a diameter of 12.70 mm (SQ samples) have failure stress values similar to the full size samples; however, when the sample diameter is reduced 21.7% from 12.70 mm to 10.00 mm (RD10 samples); the average failure stress drops from 19.8 MPa to 17.3 MPa, a 12.7% change. When the sample diameter is reduced 37.0% from 12.70 mm to 8.00 mm (RD8 samples), the average stress is reduced from 19.8 MPa to 16.9 MPa, an 14.8% change. The results are summarized in Table 7.

Table 7: Summary of percent diameter and stress reductions and grain number for all samples.

	Diameter (mm)	**% Diameter Reduction**	**Average Stress at Failure (MPa)**	**% Stress Reduction**	**Average Number of Grains Across Sample Diameter**
FS	15.875	N/A	19.1	N/A	10
SQ	12.700	N/A	19.8	N/A	8
RD10	10.000	21.7	17.3	12.7	6
RD8	8.000	37.0	16.9	14.8	5

As indicated in Table 7, a 12.70 mm diameter sample has approximately eight grains across the diameter of the specimen. Samples with 10.00 mm and 8.00 mm diameters have approximately six and five grains across the specimen diameter, respectively. Results of testing indicate that tensile strength is affected when there are fewer than eight

grains across the diameter of the test specimen. This finding for the NBG-18 graphite is in contrast with the ASTM recommendation for three to five times the maximum grain size across the tensile test specimen diameter. Based on this new information, a better recommendation would be a tensile test sample diameter that accommodates at least eight times the maximum grain size.

All cracking in graphite occurs in the binder phase due to the fact that the graphite crystals are extremely difficult to break. Graphite has no plasticity, but has fracture resistance since any cracks can be deflected from their original paths, which is common in brittle materials. The cracks may bifurcate and follow different paths around pores and grains.

The fewer grains in the graphite, the less material there is to crack through. There are also fewer ways to deflect and split a crack as well as a shorter path length. In addition, the grains may have inclusions or defects that may cause a severe stress concentration within the grain that would magnify a small stress to be within failure magnitudes. The grains themselves may also serve as stress concentrators, especially when there are only a few grains across the diameter of a sample. These situations can also lead to the reduction of stress required to break the sample.

4.4 Statistical Analysis

An Analysis of Variance (ANOVA) single factor test was conducted to determine if the difference between sample means was statistically significant or could be attributed to random sample error.

The null hypothesis states that there will be no difference between the different sample means. Specifically, the null hypothesis for the data was that all sample set means (the means of the SQ set, the FS set, the RD10 set, and the RD8 set) were equal. The null hypothesis is given by Equation 1, where μ denotes the sample set mean. The negation of the null hypothesis states that there will be a significant difference between the sample set means and is known as the alternative hypothesis. The alternative hypothesis is denoted by Equation 2.

Equation 1: The null hypothesis for the four sample sets.

$$H_0: \mu_{SQ} = \mu_{FS} = \mu_{RD10} = \mu_{RD8}$$

Equation 2: The alternative hypothesis for the four sample sets.

$$H_a: \mu_{SQ} \neq \mu_{FS} \neq \mu_{RD10} \neq \mu_{RD8}$$

The level of significance, α, was set at both 0.05 and 0.01 and represents the area in the right tail under the F-distribution curve. The level of significance is the probability of Type I error, which is error that results from falsely rejecting the null hypothesis (Schmuller 2009). This can also be stated as error attributed to determining something is statistically significant when in reality it is not.

The null hypothesis is rejected if the P-value is less than or equal to the level of significance. The P-value represents the proportion of the area of the F-distribution curve that is cut off by the F-value calculated in the ANOVA table (Schmuller 2009). In Table

8, the results for the single factor (single variable) ANOVA test are given for $\alpha = 0.05$. In Table 9, the results for the single factor ANOVA test are given for $\alpha = 0.01$. The P-value is equal to 1.57×10^{-8}, which is less than the levels of significance of 0.01 and 0.05. This allows for the rejection of the null hypothesis.

Table 8: Single factor ANOVA analysis results for $\boldsymbol{\alpha} = 0.05$.

SUMMARY

Groups	Count	Sum	Average	Variance
SQ Stress	38	751.61	19.77921	2.431126
FS Stress	40	763.55	19.08875	2.867062
RD10 Stress	19	327.89	17.25737	4.937809
RD8 Stress	18	303.51	16.86167	3.912426

ANOVA

Source of Variation	Sum of Squares	Degrees of freedom	Mean Square	F	P-value	F critical
Between Groups	150.5415	3	50.18049	15.5954	1.57E-08	2.686384
Within Groups	357.1589	111	3.217648			
Total	507.7004	114				

Table 9: Single factor ANOVA analysis results for $\boldsymbol{\alpha}$ = 0.01.

SUMMARY

Groups	Count	Sum	Average	Variance
SQ Stress	38	751.61	19.77921	2.431126
FS Stress	40	763.55	19.08875	2.867062
RD10 Stress	19	327.89	17.25737	4.937809
RD8 Stress	18	303.51	16.86167	3.912426

ANOVA

Source of Variation	Sum of Squares	Degrees of Freedom	Mean Square	F	P-value	F critical
Between Groups	150.5415	3	50.18049	15.5954	1.57E-08	3.96308
Within Groups	357.1589	111	3.217648			
Total	507.7004	114				

A planned comparison (*a priori* test) t-test formula for four samples was used to compare each sample group mean to each other in detail after the decision was made to reject the null hypothesis based on both sets of ANOVA results. The equation for the *a priori* test is labeled Equation 3. MS_W denotes the mean square deviation from the mean within the groups, c denotes a comparison coefficient, n denotes the number of samples in the group, and $\bar{x}$ denotes the group mean.

Equation 3: Planned comparison t-test for four groups (Schmuller 2009).

$$t = \frac{c_1\overline{x_1} + c_2\overline{x_2} + c_3\overline{x_3} + c_4\overline{x_4}}{\sqrt{MS_W\left[\left(\frac{c_1^2}{n_1}\right) + \left(\frac{c_2^2}{n_2}\right) + \left(\frac{c_3^2}{n_3}\right) + \left(\frac{c_4^2}{n_4}\right)\right]}}$$

The t-test determines whether or not the differences between the sample means are statistically significant. Unlike the ANOVA analysis, the t-test will indicate the specific values between which there are significant differences. ANOVA results indicate only that there is a significant difference between the means, not which of the individual means have statistically significant differences. The criterion for rejecting a t-test null hypothesis is whether the calculated F-statistic is greater than the critical value of F, which is denoted as F'. The t-test results are summarized in Table 10 and

Table **11**.

Table 10: t-test results for $\boldsymbol{\alpha}$ = 0.05.

	P-value	**t**	**F**	**F'**	**Null Hyp.**
SQ vs FS	4.60E-02	1.70	2.89	8.06	Accept
SQ vs RD10	1.06E-06	5.00	25.04	8.06	Reject
SQ vs RD8	5.37E-08	5.68	32.31	8.06	Reject
FS vs RD10	1.91E-04	3.66	13.43	8.06	Reject
FS vs RD8	1.38E-05	4.37	19.14	8.06	Reject
RD10 vs RD8	2.52E-01	0.67	0.45	8.06	Accept

Table 11: t-test results for $\boldsymbol{\alpha}$ = 0.01.

	P-value	**t**	**F**	**F'**	**Null Hyp.**
SQ vs FS	4.60E-02	1.70	2.89	11.89	Accept
SQ vs RD10	1.06E-06	5.00	25.04	11.89	Reject
SQ vs RD8	5.37E-08	5.68	32.31	11.89	Reject
FS vs RD10	1.91E-04	3.66	13.43	11.89	Reject
FS vs RD8	1.38E-05	4.37	19.14	11.89	Reject
RD10 vs RD8	2.52E-01	0.67	0.45	11.89	Accept

For both α = 0.05 and α = 0.01, the difference between the SQ sample set and the FS sample set is too small to be considered statistically significant; therefore, the null hypothesis for that individual comparison must be accepted. In addition, the difference between the RD10 and RD8 sample sets is too small to be statistically significant, which also leads to the acceptance of the null hypothesis for this individual comparison.

The null hypotheses for the comparisons between the SQ sample set and the RD10 sample set, the SQ sample set and the RD8 sample set, the FS sample set and the RD10 sample set, and the FS sample set and the RD8 sample set are rejected based on the F-statistic being greater than F'. The null hypothesis is rejected because the differences between the means are statistically significant.

5. Conclusions

The objective of research presented in this thesis was to determine whether or not there is a correlation between the tensile strength and diameter of graphite test samples.

Although a reduced load is applied to break a smaller sample, the stress should remain the same if the specimen is representing bulk material properties. Results of research described in this thesis indicate there is an effect on the tensile strength of the NBG-18 graphite specimen when the sample diameter is reduced from an original sample diameter of 12.7 mm to 10 mm and 8 mm. The correlation between sample diameter and tensile strength is not linear, but rather results suggest a diameter lower limit at which bulk material mechanical properties are no longer represented.

Graphite tends to fracture due to preexisting flaws. Cracking occurs in the binder phase and cracks can travel along different paths and bifurcate around pores or grains, which gives graphite its fracture resistance. The presence of fewer grains means less material through which to crack. As a result there are fewer paths for crack deflection or splitting and the crack path length will be shorter. This phenomenon will result in failure at a lower stress condition.

A reduction in tensile strength at fracture is seen in the experimental samples at six grains across the specimen diameter, which is above the ASTM's minimum recommendation of three to five times the maximum grain size of the specimen. It is expected, therefore, a sample of NBG-18 graphite with the ASTM recommended small diameter (6.5 mm) would exhibit similar behavior. Only four grains, on average, would traverse a 6.5-mm diameter, NBG-18 graphite sample. As such, a more appropriate

recommendation for minimum sample size would be at least eight times the maximum grain size or an approximate diameter of 12.7 mm for grade NBG-18 graphite.

It is of interest to consider the implications of this research for the NGNP, for which NBG-18 graphite is proposed as fuel block material. The fuel block design includes graphite webbing 2 to 3 mm thick. Conclusions of this thesis imply a reduction in the tensile strength of non-irradiated NBG-18 graphite at thicknesses less than 10 mm. The effect on irradiated graphite tensile strength is unknown.

6. Future Work

Further work is needed to characterize other kinds of graphites that are also candidates for the VHTR. Perhaps another grade of graphite has a different grain size effect than does NBG-18. Given that IG-110 has very fine grains, perhaps its threshold diameter is much smaller than that of NBG-18. Perhaps graphites with different kinds of cokes and binders will also have different grain size effects and different characteristic fracture mechanics.

In addition, the grain size effect should be studied on irradiated samples as it is unknown how small irradiated samples will perform mechanically. Will the graphite disintegrate more quickly on an area of only a few grains versus an area of thousands of grains? Will the irradiation damage mechanism change? These are subjects for future studies.

Appendix 1
Works Cited

Antolovich, Stephen D., and Bruce F. Antolovich. "An Introduction to Fracture Mechanics." In *ASM Handbook, Volume 19: Fatigue and Fracture*, by ASM Handbook Committee, 371-380. 1996.

ASTM International. *ASTM C 781: Standard Practice for Testing Graphite and Boronated Graphite Materials for High-Temperature Gas-Cooled Nuclear Reactor Components.* ASTM Standard, West Conshohocken: ASTM International, 2008.

Barson, John M., and Stanley T. Rolfe. "Stress Analysis for Members with Cracks--KI." In *Fracture and Fatigue Control in Structures--Applicaions of Fracture Mechanics: (MNL 41)*, 28-64. ASTM International, 1999.

Burchell, T., R. Bratton, and W. Windes. *NGNP Graphite Selection and Acquisition Strategy.* Oak Ridge: Oak Ridge National Laboratory, 2007.

Burchell, T., R. L. Bratton, R. N. Wright, and J. Wright. *Project #23747, Next Generation Nuclear Plant Materials Research and Development Program Plan, PLN-2674.* Idaho Falls: Idaho National Laboratory, 2007.

Burchell, T.D., and L.L. Snead. "The effect of neutron irradiation damage on the properties of grade NBG-10 graphite." *Journal of Nuclear Materials*, no. 371 (2007): 18-27.

Burchell, Tim, Steve Nunn, Joe Strizak, and Marie Williams. "AGC-1 Sister Specimen Testing Data Report." Oak Ridge, 2009.

Burchell, Timothy D. *Thermal Properties and Nuclear Energy Applications.* Vol. 1, chap. 5 in *Graphite and Precursors: World of Carbon*, edited by Pierre Delhaes, 87-109. Amsterdam: Gordon and Breach Science Publishers, 2001.

Carroll, M.C., W.D. Swank, and W.E. Windes. "Optimization of Tensile Testing of Cylindrical Graphite Specimens." 2009.

Chung, D.D.L. "Review Graphite." *Journal of Materials Science*, no. 37 (2002): 1475-1489.

De Halas, D.R. "Theory of Radiation Effects in Graphite." Chap. 7 in *Nuclear Graphite*, by R.E. Nightingale, 195-237. New York: Academic Press, 1962.

DOE-NE. *Next Generation Nuclear Plant: A Report to Congress.* U.S. Department of Energy, Office of Nuclear Energy, 2010.

Dresselhaus, M.S., G. Dresselhaus, and R. Saito. *Electronic Band Structure of Graphite.* Vol. 1, chap. 2 in *Graphite and Precursors, World of Carbon*, edited by Pierre Delhaes, 25-43. Amsterdam: Gordon and Breach Science Publishers, 2001.

Eatherly, W.P., and E.L. Piper. "Manufacture." Chap. 2 in *Nuclear Graphite*, by R.E. Nightingale, 21-51. New York: Academic Press, 1962.

Gross, Todd S. "Micromechanisms of Monotonic and Cyclic Crack Growth." In *ASM Handbook, Volume 19: Fatigue and Fracture*, by ASM Handbook Committee, 42-60. 1996.

Huston, Ronald, and Harold Josephs. *Practical Stress Analysis in Engineering Design.* 3rd Edition. CRC Press, 2009.

Idaho National Laboratory. *Next Generation Nuclear Plant Intermediate Heat Exchanger Materials Research and Development Plan, PLN-2804.* Idaho Falls: Idaho National Laboratory, 2008.

Kelly, B.T. *Physics of Graphite.* Englewood, NJ: Applied Science Publishers INC, 1981.

Nichols, P.F., and E.M. Woodruff. "Nuclear Properties." Chap. 4 in *Nuclear Graphite*, by R.E. Nightingale, 67-85. New York: Academic Press, 1962.

Nightingale, R. E. "Graphite in Nuclear Industry." In *Nuclear Graphite*, by R. E. Nightingale, 1-20. New York: Academic Press, 1962.

Pierson, H.O. *Handbook of Carbon, Graphite, Diamond and Fullerenes: Properties, Processing, and Applications.* Park Ridge, NJ: Noyes Publications, 1993.

Pitner, A.L. "Irradiation Behavior of Poco Graphites." *Carbon* (Pergamon Press) 9 (1971): 637-644.

Rand, Brian. *Mechanical Properties.* Vol. 1, chap. 6 in *Graphite and Precursors, World of Carbon*, edited by Pierre Delhaes, 111-139. Amsterdam: Gordon and Breach Science Publishers, 2001.

Schmuller, Joseph. *Statistical Analysis with Excel For Dummies.* Hoboken: Wiley Publishing, Inc., 2009.

Snead, L.L., T. D. Burchell, and Y. Katoh. "Swelling of Nuclear Graphite and High Quality Carbon Fiber Composite Under Very High Irradiation Temperature." *Journal of Nuclear Materials*, no. 381 (2008): 55-61.

T. Burchell, R. Bratton, W. Windes. *NGNP Graphite Slection and Acqusition Strategy.* Oak Ridge: Oak Ridge National Laboratory, 2007.

William D. Callister, Jr. *Materials Science and Engineering: An Introduction.* New York: John Wiley & Sons, 1994.

Windes, W., T. Burchell, and R. Bratton. *Project #23747, Graphite Technology Development Plan, PLN-2497.* Idaho Falls: Idaho National Laboratory, 2007.

Windes, William. Idaho Falls, October 28, 2010.

Appendix 2
Experimental Data

Table 12: Experimental Data

Sample	Strain to Failure (%)	Stress (MPa)	Break Code	Break Msrmnt (mm) (B-T)	S.T.F. Std Dev	Stress Std. Dev	
1	0.22921	21.41	N/A	N/A	0.042550928	0.955546964	
2	0.51764	19.92	N/A	N/A	0.24902	20.99800	Average
3	0.19780	20.83	N/A	N/A	17.08749085	4.550657033	Percentage
4	0.27835	22.35	N/A	N/A			
5	0.23453	19.78	3	4.05			
6	0.30520	20.62	1	21.35			
SQ1	0.22685	20.54	1	21.57	0.073849448	1.559206974	
SQ2	0.39945	19.52	3	4.52	0.25788	19.77921	Average
SQ3	0.21583	20.49	1	22.39	28.63751656	7.883059699	Percentage
SQ4	0.27709	20.86	2	6.03			
SQ5	0.11811	17.88	1	24.39			
SQ6	0.20150	21.60	3	6.18			
SQ7	0.19315	17.42	2	8.52			
SQ8	0.29661	20.20	3	3.35			
SQ9	0.45260	18.33	2	18.47			
SQ10	0.21882	18.55	1	23.79			
SQ11	0.33921	19.52	1	23.54			
SQ12	0.18228	20.74	2	17.96			
SQ13	0.21465	21.44	1	24.15			
SQ14	0.25394	19.76	1	23.74			
SQ15	0.20268	18.64	3	4.15			
SQ16	0.30409	16.76	2	13.43			
SQ17	0.20898	20.45	2	18.67			
SQ18	0.24843	20.45	1	22.65			
SQ19	0.28520	20.41	3	4.73			
SQ20	0.21772	20.13	3	3.69			
SQ21	0.18031	20.73	3	3.18			
SQ22	0.15331	18.61	2	8.08			
SQ23	0.35929	14.96	2	6.68			
SQ24	0.13150	21.48	3	4.46			
SQ25	0.22874	20.05	2	18.93			
SQ26	0.28291	17.65	2	9.16			
SQ27	0.26488	22.38	1	23.43			
SQ28	0.32591	18.42	2	5.82			
SQ29	0.27213	22.07	3	4.14			
SQ30	0.19913	21.48	2	18.33			
SQ31	0.26331	21.09	1	23.67			
SQ32	0.40866	20.83	2	20.17			
SQ33	0.31685	20.72	1	22.74			
SQ34	0.22094	19.25	1	22.95			
SQ35	0.30331	19.66	1	23.00			
SQ36	0.31551	20.43	1	23.12			
SQ37	0.24102	18.53	1	22.54			
SQ38	0.27441	19.58	2	10.35			

FS1	0.24900	19.03	N/A	N/A	0.026185127	1.693240237	
FS2	0.24800	19.08	N/A	N/A	0.26033	19.08875	Average
FS3	0.26900	19.05	N/A	N/A	10.05862956	8.870356817	Percentage
FS4	0.22900	17.80	N/A	N/A			
FS5	0.27000	20.61	N/A	N/A	With Grain		
FS6	0.27600	20.10	N/A	N/A	0.023002231	1.653835335	
FS7	0.24600	19.35	N/A	N/A	0.25705	19.14350	Average
FS8	0.25200	18.41	N/A	N/A	8.948543479	8.639148197	Percentage
FS9	0.33400	21.09	N/A	N/A			
FS10	0.23600	18.29	N/A	N/A	Against Grain		
FS11	0.26200	18.16	N/A	N/A	0.0292528	1.773003399	
FS12	0.22300	16.80	N/A	N/A	0.26360	19.03400	Average
FS13	0.25500	17.64	N/A	N/A	11.09742039	9.314928018	Percentage
FS14	0.21600	15.62	N/A	N/A			
FS15	0.22000	16.16	N/A	N/A			
FS16	0.28900	21.58	N/A	N/A			
FS17	0.24100	18.76	N/A	N/A			
FS18	0.27700	20.24	N/A	N/A			
FS19	0.29000	21.00	N/A	N/A			
FS20	0.28600	21.38	N/A	N/A			
FS21	0.20500	15.67	N/A	N/A			
FS22	0.28400	22.23	N/A	N/A			
FS23	0.24800	17.71	N/A	N/A			
FS24	0.29100	18.71	N/A	N/A			
FS25	0.27100	20.18	N/A	N/A			
FS26	0.26900	20.74	N/A	N/A			
FS27	0.24800	18.94	N/A	N/A			
FS28	0.28400	20.28	N/A	N/A			
FS29	0.26600	17.07	N/A	N/A			
FS30	0.28300	20.21	N/A	N/A			
FS31	0.25300	18.36	N/A	N/A			
FS32	0.23800	17.74	N/A	N/A			
FS33	0.22000	16.73	N/A	N/A			
FS34	0.25700	18.98	N/A	N/A			
FS35	0.27600	19.41	N/A	N/A			
FS36	0.26100	18.55	N/A	N/A			
FS37	0.24200	19.20	N/A	N/A			
FS38	0.28400	21.56	N/A	N/A			
FS39	0.29400	21.83	N/A	N/A			
FS40	0.27100	19.30	N/A	N/A			
RD1	0.194	17.1	N/A	N/A	0.152199454	1.306672638	10 mm
RD2	0.169	11.4	N/A	N/A	0.302010118	17.87058824	Average
RD3	0.22591	18.61	N/A	N/A	50.39548171	7.31186137	Percentage
RD4	0.23638	16.04	N/A	N/A			
RD5	0.19083	12.69	N/A	N/A			
RD6	0.18024	17.89	N/A	N/A			
RD7	N/A	N/A	N/A	N/A			
RD8	0.16543	17.4	N/A	N/A			
RD9	0.26614	19.56	N/A	N/A			
RD10	0.2663	16.29	N/A	N/A			
RD11	0.2974	18.73	N/A	N/A	0.079626176	1.682186952	8 mm
RD12	0.25811	17.35	N/A	N/A	0.276894118	16.59823529	Average
RD13	0.22622	15.72	N/A	N/A	28.75690411	10.13473374	Percentage
RD14	0.34409	15.53	N/A	N/A			
RD15	0.22299	15.88	N/A	N/A			
RD16	0.21354	16.64	N/A	N/A			
RD17	0.29598	15.62	N/A	N/A			
RD18	0.26362	17.8	N/A	N/A			
RD19	0.29472	14.73	N/A	N/A			
RD20	0.25945	13.9	N/A	N/A			
RD21	0.34173	18.61	N/A	N/A			
RD22	0.20063	19.24	N/A	N/A			
RD23	0.30591	19.71	N/A	N/A			
RD24	0.57134	16.59	N/A	N/A			
RD25	0.26449	19.23	N/A	N/A			
RD26	0.52866	17.8	N/A	N/A			
RD27	0.66882	18.01	N/A	N/A			
RD28	0.101732	18.31	N/A	N/A			
RD29	0.28701	18.29	N/A	N/A			
RD30	0.32945	15.12	N/A	N/A			

RD33	0.21039	13.18	N/A	N/A			
RD34	N/A	N/A	N/A	N/A			
RD35	0.15299	19.46	N/A	N/A			
RD36	0.30094	17.27	N/A	N/A			
RD37	0.20417	17.99	N/A	N/A			
RD38	0.5111	17.27	N/A	N/A			
RD39	0.33669	17.41	N/A	N/A			
RD40	0.41906	21.34	N/A	N/A			
					Average	Average	
Total Std Dev	0.0972	2.3036		1 = Top	0.27504	19.01000	Gauge Break
Average Value	0.2708	18.6000		2 = Gauge	0.25078	20.04600	Top Break
Total Std. Dev. %	35.8776	12.3851		3 = Bottom	0.24301	20.53111	Bottom Break
					Std Dev	Std Dev	
For All Small Samples					0.08874	1.88357	Gauge Break
					0.05491	1.19689	Top Break
					0.07932	1.08019	Bottom Break
					For SQ Samples Only		